Chinese Journal of Natural Medicines

Periplaneta americana* extract promotes infectious diabetic ulcers wound healing by downregulation of *LINC01133/SLAMF9

Yuhang YANG, Jun HUANG, Xintian LI, Renjing LIN, Xiaoyan WANG, Ge XIAO, Juanni ZENG, Zhenquan WANG

Citation: Yuhang YANG, Jun HUANG, Xintian LI, Renjing LIN, Xiaoyan WANG, Ge XIAO, Juanni ZENG, Zhenquan WANG, *Periplaneta americana* extract promotes infectious diabetic ulcers wound healing by downregulation of *LINC01133/SLAMF9*, Chinese Journal of Natural Medicines, 2024, 22(7), 608−618. doi: 10.1016/S1875−5364(24)60569−8.

View online: https://doi.org/10.1016/S1875−5364(24)60569−8

Available online at www.sciencedirect.com
ScienceDirect
Chinese Journal of Natural Medicines 2024, **22**(7): 608-618
doi: 10.1016/S1875-5364(24)60569-8
Chinese Journal of Natural Medicines

•Original article•

Periplaneta americana extract promotes infectious diabetic ulcers wound healing by downregulation of *LINC01133*/*SLAMF9*

YANG Yuhang[1Δ], HUANG Jun[1Δ], LI Xintian[1], LIN Renjing[1], WANG Xiaoyan[1], XIAO Ge[1], ZENG Juanni[1, 3*], WANG Zhenquan[2*]

[1] *Department of Anorectal Disease 1, The Second Affiliated Hospital of Hunan University of Traditional Chinese Medicine, Changsha 410005, China;*
[2] *Department of Anorectal Disease 3, The Second Affiliated Hospital of Hunan University of Traditional Chinese Medicine, Changsha 410005, China;*
[3] *Laboratory of Vascular Biology and Translational Medicine, Medical School, Hunan University of Chinese Medicine/Hunan Provincial Key Laboratory of Vascular Biology and Translational Medicine , Changsha 410208, China*

Available online 20 Jul., 2024

[ABSTRACT] Wound healing in diabetic ulcers remains a significant clinical challenge, primarily due to bacterial infection and impaired angiogenesis. *Periplaneta americana* extract (PAE) has been widely used to treat diabetic wounds, yet its underlying mechanisms are not fully understood. This study aimed to elucidate these mechanisms by analyzing long non-coding RNA (lncRNA) expressions in the wound tissues from diabetic anal fistula patients treated with or without PAE, using high-throughput sequencing. Peripheral blood monocytes from patients were differentiated into M0 macrophages with human macrophage colony-stimulating factor (hM-CSF) and subsequently polarized into M1 macrophages with lipopolysaccharide. The results indicated that *LINC01133* and *SLAMF9* were downregulated in wound tissues of patients treated with PAE. Furthermore, PAE suppressed M1 macrophage polarization and enhanced human umbilical vein endothelial cell (HUVEC) proliferation, migration, and angiogenesis. These effects were diminished when *LINC01133* or *SLAMF9* were overexpressed. Mechanistically, *LINC01133* was shown to upregulate *SLAMF9* through interaction with *ELAVL1*. Overexpression of *SLAMF9* reversed the effects of *LINC01133* silencing on macrophage polarization and HUVEC functions. In conclusion, PAE facilitates the healing of infected diabetic ulcers by downregulating the *LINC01133*/*SLAMF9* pathway.

[KEY WORDS] *Periplaneta americana* extract; Infectious diabetic ulcers; M1 macrophage polarization; *LINC01133*; *SLAMF9*
[CLC Number] R965 **[Document code]** A **[Article ID]** 2095-6975(2024)07-0608-11

Introduction

Diabetic ulcers represent a severe complication of diabetes mellitus, resulting in chronic non-healing wounds [1]. Despite employing various therapeutic strategies such as regular debridement, revascularization, and anti-infection treatments [2], managing diabetic wounds remains challenging. In normal tissues, wound healing encompasses key phases, including inflammation, proliferation, and tissue remodeling [3], which involve intricate interactions among various cells, such as macrophages and endothelial cells [4]. In contrast, diabetic wound healing is frequently impaired, with issues such as insufficient angiogenesis and prolonged inflammation [5]. A critical aspect of this dysfunction is the persistent and dysregulated M1 macrophage polarization, which promotes inflammation [6]. Consequently, there is a pressing need to develop novel therapeutic agents and to elucidate their molecular mechanisms in modulating the impaired healing processes, thereby contributing to more effective treatments for diabetic ulcers.

Previous research has highlighted the potential of the medicinal insect *Periplaneta americana* as a therapeutic agent for diabetic skin ulcers. Glycoproteins and protein-polysaccharide complexes isolated from *P. americana* effectively promote diabetic wound healing [7, 8]. Kangfuxin Liquid, a solution derived from *P. americana* extract (PAE), contains bioactive substances such as peptides, various growth

[Received on] 15-Jan.-2024
[Research funding] This work was supported by the Natural Science Foundation of Hunan Province (No. 2021JJ30516).
[*]**Corresponding author]** E-mails: juannizeng1239@163.com (ZENG Juanni); wangzhenquan123456@163.com (WANG Zhenquan)
[Δ]These authors contributed equally to this work.
These authors have no conflict of interest to declare.

factors, amino acids, polyols, and mucous acids [9] and is widely used in clinical practice for treating diabetic skin ulcers [10]. Despite its clinical use, the specific protective mechanisms by which PAE improves diabetic skin ulcers remain largely obscure. PAE has been shown to exert protective effects on ulcerative diseases by regulating gene expression [11, 12]. Recent studies have established that long non-coding RNAs (lncRNAs) are critical in diabetic wound healing [13]. For instance, the reduction of lncRNA GAS5 enhances diabetic wound healing [14], and lncRNA H19 accelerates wound healing in diabetic foot ulcers [15]. Long intergenic non-coding RNA 01133 (*LINC01133*) is a recently identified lncRNA initially recognized as an oncogene in lung squamous cell carcinoma. It has since been found to be dysregulated in various types of tumors [16]. Overexpression of *LINC01133* inhibits cell proliferation and migration in gastric cancer [17] and nasopharyngeal carcinoma [18]. However, its expression and role in diabetes-related diseases remain unclear. Further research is needed to elucidate the potential involvement of *LINC01133* in the pathophysiology of diabetic ulcers and its possible therapeutic implications.

Signaling lymphocyte activation molecule family member 9 (*SLAMF9*) is part of the SLAM immunoreceptor family [19] and serves as a potential target for inflammatory diseases [20]. *SLAMF9* promotes inflammatory responses *via* specific subsets of antigen-presenting cells [21]. Deficiencies in *SLAMF8* and *SLAMF9* suppress the secretion of inflammatory cytokines and reduce the infiltration of inflammatory cells [22]. In a scratch assay using RAW 264.7 cells, a murine macrophage-like cell line, *SLAMF9*, was shown to delay wound closure [23]. Starbase predicts that ELAV-like RNA-binding protein 1 (*ELAVL1*) is a common RNA-binding protein (RBP) for both *LINC01133* and *SLAMF9*. *ELAVL1* has been implicated in diabetes-related diseases; for instance, knocking down *ELAVL1* can alleviate diabetic osteoporosis [24]. In ventricular cardiomyocytes, microRNA-9 targets *ELAVL1* to reduce hyperglycemia-induced pyroptosis [25]. Additionally, lncRNA *MALAT1* targets microRNA-23c to elevate *ELAVL1* expression, thereby regulating diabetic nephropathy [26]. Previous studies have shown that lncRNAs can regulate downstream target proteins through *ELAVL1*. For example, *LINC01119* binds with *ELAVL1* to increase the mRNA stability of brain-derived neurotrophic factor (*BDNF*) and upregulate its expression in peripheral nerve injury [27]. Similarly, lncRNA *MALAT1* destabilizes phosphatase and tensin homolog (*PTEN*) mRNA by interacting with *ELAVL1* in gastric cancer [28]. Based on these findings, we hypothesized that *LINC01133* might regulate *SLAMF9* expression *via* *ELAVL1*. However, no relevant literature currently supports this, necessitating further investigation.

In this study, we used high-throughput sequencing technology to investigate the role of *LINC01133* in the efficacy of PAE in wound healing of infectious diabetic ulcers. We validated that PAE suppresses M1 macrophage polarization and promotes human umbilical vein endothelial cell (HUVEC) proliferation, migration, and angiogenesis by downregulating the *LINC01133*/*SLAMF9* axis. These findings suggest that the *LINC01133*/*SLAMF9* axis pathway could be a key regulatory mechanism underlying the therapeutic effects of PAE in treating infectious diabetic ulcers.

Materials and Methods

Clinical samples

A total of 30 wound tissue samples were collected from diabetic anal fistula patients (45–65 years) receiving treatment with or without PAE at the Second Affiliated Hospital of Hunan University of Traditional Chinese Medicine (n = 15 per group). After local anesthesia with lidocaine, tissue samples were obtained from the non-healing edges of wounds using a 4 mm biopsy punch and were immediately flash-frozen in liquid nitrogen. Inclusion criteria were as follows: confirmed diagnosis of diabetes mellitus with anal fistula [29]; no abnormal anal morphology or function; no previous surgical intervention for anorectal disease; and a wound area between 4 and 30 cm^2. Exclusion criteria included serious diseases of vital organs (such as malignant tumors, stroke, heart failure, renal failure, and abnormal liver function), any ongoing medical therapies; known allergies to experimental or standard medications, significant mental disorders, and pregnancy or lactation. This study was approved by the Ethics Committee of the Second Affiliated Hospital of Hunan University of Traditional Chinese Medicine (No. 2022-KY-003). Written informed consent was obtained from all participants.

High-throughput sequencing of lncRNAs

Total RNA was extracted from the tissue samples using TRIzol® Reagent (#15596026CN, Invitrogen, Carlsbad, CA, USA). The concentration, purity, and integrity of the extracted RNA were assessed. For RNA sample preparation, the Ribo-Zero Magnetic kit (#RZNB1056, EpiCentre Biotechnologies, Madison, WI, USA) was used to remove rRNA from the total RNA. The rRNA-depleted RNA was then used to prepare RNA libraries with the TruSeq™ Stranded Total RNA Library Prep Kit (#RS-122-2002, Illumina, San Diego, CA, USA). High-throughput sequencing was performed using the HiSeq 4000 SBS Kit (#FC-410-1003, Illumina). To analyze the preliminarily screened lncRNAs, four software tools were employed: PLEK version 1.2, CPAT version 3.0.4, CNCI version 2 (Chinese Academy of Sciences, China), and CPC2 version 2 (BioInformation Center, Peking University, School of Life Sciences, State Key Laboratory of Protein and Plant Gene Research, China). Differentially expressed lncRNAs were visualized using a Volcano plot.

Cell culture

Peripheral blood mononuclear cells (PBMCs) were collected from diabetic anal fistula patients and healthy volunteers. $CD14^+$ cells were enriched using magnetic-activated cell sorting columns (#19059, EasySep, Stem Cell, Vancouver, BC, Canada). M0 macrophages, or immature macrophages, were differentiated from PBMCs by treatment with

human macrophage colony-stimulating factor (#M6518, hM-CSF, 30 ng·mL^{-1}, Sigma, St. Louis, MO, USA) for 7 d. The cells were maintained in RPMI-1640 medium (#11875093, Gibco, Grand Island, NY, USA) supplemented with 10% fetal bovine serum (FBS, #10099158, Gibco). To induce M1 macrophage activation, the cells were incubated with 200 ng·mL^{-1} lipopolysaccharide (LPS, #L2880, Sigma) for 24 h. Human umbilical vein endothelial cells (HUVEC, #PCS-100-010) and human embryonic kidney 293 cells (HEK293, #CRL-1573) were obtained from the American Type Culture Collection (Manassas, VA, USA). These cells were cultured in Dulbecco's Modified Eagle Medium (DMEM) supplemented with 10% FBS (Gibco) and 1% penicillin/streptomycin (#P4333, Gibco). All cells were maintained in a 5% CO_2 atmosphere at 37 °C. For actinomycin D treatment, HUVECs were exposed to actinomycin D (2 μg·mL^{-1}, #SBR00013, Sigma) for 0, 4, 8 or 12 h.

Cell transfection

Overexpression plasmids, including pcDNA3.1-*LINC01133* (Oe-*LINC01133*) and pcDNA3.1-*SLAMF9* (Oe-*SLAMF9*), as well as short hairpin RNA (shRNA) *LINC01133* (sh-*LINC01133*) and *ELAVL1* (sh-*ELAVL1*), along with their corresponding negative controls, were obtained from GenePharma (Shanghai, China). Cells were seeded in 12-well plates and cultured for 24 h. Following the manufacturer's protocol, transfection was conducted using Lipofectamine 300 (#L3000150, Invitrogen). After 48 h, cells were collected for subsequent experiments.

Flow cytometry

The expressions of *CD11b* and *CD86* were evaluated by flow cytometry. Cells were fixed in 4% formaldehyde for 10 min and then resuspended in 2% FBS. They were incubated with *CD11b* antibody conjugated with phycoerythrin (PE) (#12-0118-42, 1∶20, eBioscience, San Diego, CA, USA) or *CD86* antibody conjugated with fluorescein isothiocyanate (FITC) (#MA1-35969, 1∶20, Invitrogen) for 30 min. The cells were then analyzed using a FACScan flow cytometer (Becton Dickinson, Franklin Lakes, NJ, USA).

Cell viability assessment

Cell viability was measured using the Cell Counting Kit 8 (CCK-8) (#CA1210, Solarbio, Beijing, China). Cells (4×10^3/well) were seeded in a 96-well plate. Following the specified treatments, the culture medium was discarded, and 10 μL of CCK-8 solution (5 mg·mL^{-1}) was added to each well for 2 h at 37 °C. Optical density (OD) at 450 nm was detected using a spectrophotometer (Synergy H1, BioTek, Winooski, VT, USA).

Cell scratch assay

Cells (5.0×10^4 cells/well) were seeded in a 6-well plate and cultured overnight. A sterile 200 μL pipette tip was used to create uniform scratches (wounds) in each well. The cells were then rinsed with PBS before being treated with the indicated agents. After staining with crystal violet, images of the cells were captured at 0 and 24 h. The cell migration rate was calculated using the formula: Cell migration rate (%) = [(scratch area at 0 h – scratch area at 24 h)/scratch area at 0 h] × 100%. Scratch areas were quantitatively analyzed using ImageJ software (version 2.0, NIH, Bethesda, MD, USA).

Endothelial cell tube formation

Following the indicated treatments, HUVECs (1.0×10^4 cells/well) were seeded in an angiogenesis μ-slide (#81506, ibidi, Martin Reid, Germany) precoated with 10 μL of basement membrane matrix (#354230, Corning, Bedford, MA, USA). After 6 h, images of capillary-like tube structures were captured using a light microscope. The length and number of intact tubes per field were analyzed using ImageJ software.

Enzyme-linked immunosorbent assay (ELISA)

Cells (1×10^6 cells/well) were pretreated with the indicated reagents, and the supernatants were collected. Following the manufacturer's protocol, the concentrations of tumor necrosis factor-alpha (TNF-α) (#HSTA00E) and interleukin 6 (IL-6) (#HS600C) in the cell supernatants were measured using ELISA kits (R&D Systems, Minneapolis, MN, USA). Absorbance at 450 nm was determined using a microplate reader (iMark, BioRad, Hercules, CA, USA).

RNA immunoprecipitation

Cells were lysed using a lysis buffer, and the lysate was centrifuged to collect the supernatant. Samples were incubated with an IgG antibody (ab172730, 1∶30, Abcam, Cambridge, MA, USA) or an *ELAVL1* antibody (ab200342, 1∶30, Abcam, Cambridge, UK) along with magnetic beads coupled with protein A/G, followed by overnight incubation at 4 °C. The magnetic bead-protein-RNA complexes were then washed and purified for subsequent reverse transcription-quantitative polymerase chain reaction (RT-qPCR) analysis.

RNA pull-down assay

A biotinylated-*SLAMF9* probe (bio-*SLAMF9*) was obtained from Sangon Biotech (Shanghai, China). After cell lysis and centrifugation, the lysates were incubated with an oligo probe or *SLAMF9* probe at room temperature for 2 h. Streptavidin magnetic beads (#LSKMAGT, Sigma) were then added and incubated at room temperature for 1 h. The RNeasy Mini Kit (#74104, Qiagen, Hilden, Germany) was used to purify and isolate the RNA coupled with the magnetic beads. The enrichment of *ELAVL1* was finally detected by RT-qPCR.

Reverse transcription-quantitative polymerase chain reaction (RT-qPCR)

Total RNA was extracted from tissues or cells using an RNA isolation reagent (AM1914, Invitrogen). The cDNA was synthesized using the PrimeScript™ RT Master Mix (#RR036A, Takara, Tokyo, Japan). qPCR was performed on a 7500 FAST Real-Time PCR System (Applied Biosystems, Foster City, CA, USA) using SYBR Green PCR Master Mix (#4309155, Applied Biosystems). Primers used are listed in Table 1 with *β-Actin* serving as the reference gene. The relative gene expressions were calculated using the $2^{-\Delta\Delta Ct}$ method.

Western blotting analysis

Cells were lysed using RIPA lysis buffer (#P0013,

Table 1 Primer sequences used in RT-qPCR

Gene	Forward primer (5′-3′)	Reversed primer (5′-3′)
LINC01133	GCTGTGGTGGAGAGAATGGA	CCCCAGCTTTCCAGATCCAAA
SLAMF9	CACAAGTCAGTGCGGTTCAC	GTGTTTCCTGTGTTAATGCCAC
ELAVL1	TGTTCTCTCGGTTTGGGCGGAT	TCTTCTGCCTCCGACCGTTTGT
β-Actin	TGGCACCACACCTTCTACAA	CCAGAGGCGTACAGGGATAG

Beyotime, Jiangsu, China). Protein concentrations were measured with the Pierce™ BCA Protein Assay Kit (#23225, Thermo Fisher Scientific). Proteins were separated by SDS-PAGE and transferred onto PVDF membranes (#ISEQ00005, Millipore, Bedford, MA, USA). The membranes were blocked with 5% skimmed milk at room temperature for 1 h, followed by overnight incubation at 4 °C with primary antibodies, including anti-*SLAMF9* (SAB3500718, 1∶500, Sigma) and anti-*ELAVL1* (ab200342, 1∶1000, Abcam). Subsequently, the membranes were incubated with secondary antibodies at room temperature for 2 h. Immunoblots were visualized using ECL reagent (#32209, Thermo), and protein levels were quantified using ImageJ software.

Statistical analysis

Data were analyzed using SPSS 21.0 software (IBM, Armonk, NY, USA) and presented as mean ± standard deviation (SD). Experiments were conducted in triplicate. The Pearson correlation coefficient was used to assess the correlation between *LINC01133* and *SLAMF9* expression levels. Comparisons among multiple groups were performed using one-way ANOVA followed by Tukey's post hoc test. Comparisons between two groups were conducted using Student's *t*-test. A *P* value of < 0.05 was considered statistically significant.

Results

Downregulation of LINC01133 and SLAMF9 in diabetic anal fistula patients treated with PAE

To elucidate the impact of PAE treatment on gene expression in diabetic anal fistula patients, we collected wound tissues from patients receiving PAE treatment and those not receiving the treatment for high-throughput sequencing analysis. A Volcano plot was generated to identify differentially expressed lncRNAs, revealing a significant downregulation of *LINC01133* in the wound tissues of PAE-treated patients (Fig. 1A). Subsequent RT-qPCR analysis validated these findings, showing that both *LINC01133* and *SLAMF9* mRNA levels were significantly reduced in the wound tissues of PAE-treated patients (Fig. 1B). These results suggest that the downregulation of *LINC01133* and *SLAMF9* may be involved in the wound healing process in infectious diabetic ulcers.

PAE suppresses M1 macrophage polarization and promotes HUVEC proliferation, migration, and angiogenesis

Previous studies have shown that diabetic wounds are characterized by persistent and dysregulated M1 macrophage polarization [6] and impaired angiogenesis, which are major obstacles to healing [30]. To further investigate the effects of PAE on these processes, we examined its impact on macro-

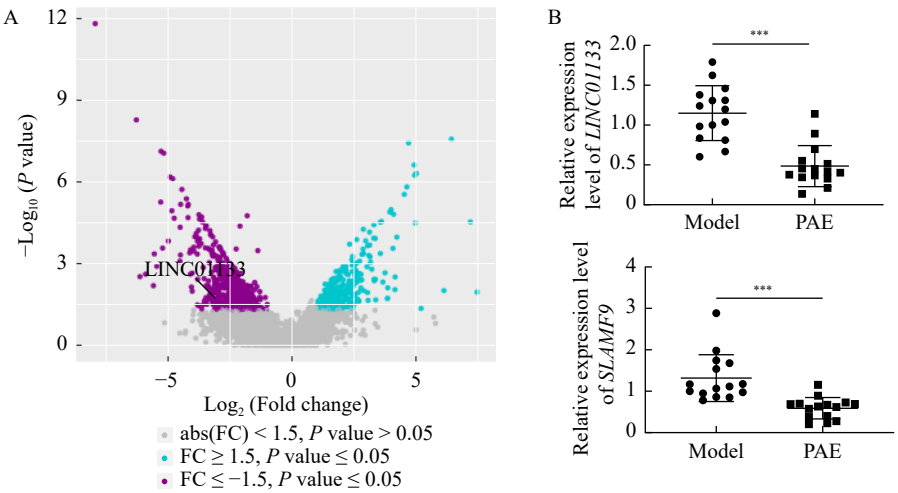

Fig. 1 *LINC01133* and *SLAMF9* were downregulated in diabetic perianal fistula patients treated with PAE. Wound tissues were obtained from diabetic anal fistula patients with or without PAE treatment. (A) Volcano plot was used to analyze the differentially expressed lncRNAs in patients with or without PAE treatment. Blue spots represented upregulated lncRNAs ($P < 0.05$), purple spots indicated downregulated lncRNAs ($P < 0.05$), and gray spots represented lncRNAs that did not present significant alterations ($P > 0.05$). (B) The expressions of *LINC01133* and *SLAMF9* mRNA were measured with RT-qPCR. Data are presented as the mean ± SD ($n = 15$ per group). $^{***}P < 0.001$.

phage polarization, HUVEC proliferation, migration, and angiogenesis. PBMCs were isolated from healthy volunteers and diabetic anal fistula patients. PBMCs from diabetic patients were then treated with PAE. Flow cytometry analysis revealed no significant differences in the macrophage marker *CD11b* among the three groups. However, *CD86* (an M1 macrophage marker) was significantly elevated in the model group compared to the normal group, and this increase was significantly reduced in the PAE-treated group (Fig. 2A). Furthermore, the mRNA levels of *LINC01133* and *SLAMF9* in PBMC were upregulated in the model group but downregulated in the PAE-treated group (Fig. 2B). For further analysis, PBMCs from diabetic anal fistula patients were differentiated into M0 macrophages using hM-CSF, followed by LPS stimulation to induce M1 polarization. These cells were then treated with PAE. Compared to the control group, LPS-treated cells showed increased levels of CD86, IL-6, and TNF-α, which were progressively reduced with increasing concen-

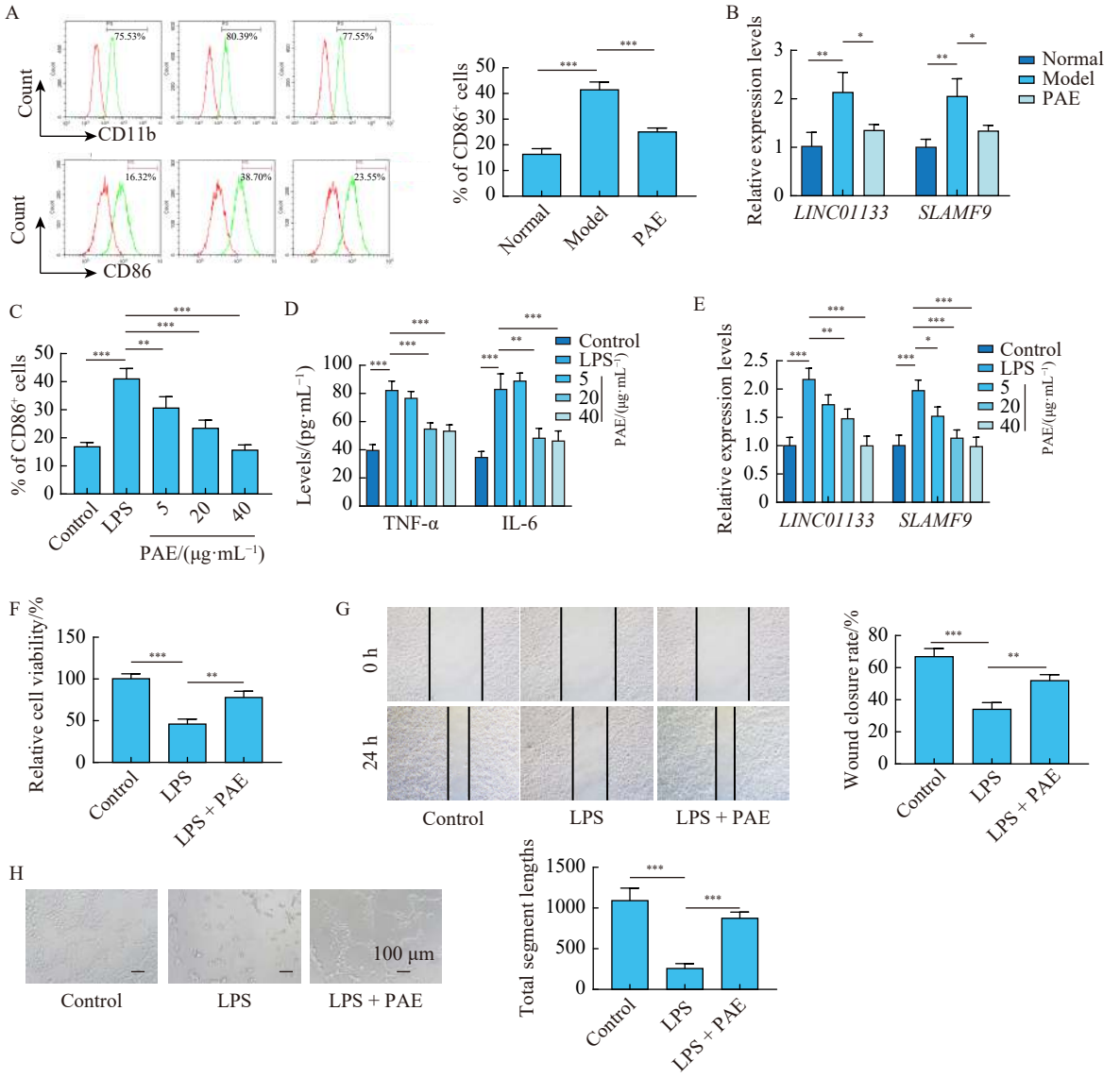

Fig. 2 PAE inhibited M1 macrophage polarization and promoted HUVEC proliferation, migration, and angiogenesis. (A, B) Peripheral blood was collected from healthy individuals or diabetic perianal fistula patients with or without PAE treatment. PBMC were isolated and differentiated into macrophages by hM-CSF. (A) Identification of macrophage markers (CD11b and CD86) with flow cytometry. (B) *LINC01133* and *SLAMF9* mRNAs were detected using RT-qPCR. (C, D) LPS induced the M1 polarization of macrophages derived from diabetic anal fistula patients, and then PAE (5, 20, or 40 μg·mL^{-1}) was addd into the macrophages. (C) M1 macrophage marker (CD86) was identified by flow cytometry. (D) Inflammatory cytokines were detected with ELISA. (E) *LINC01133* and *SLAMF9* mRNA levels were determined using RT-qPCR. (F−H) HUVECs were co-cultured with macrophages, followed by incubation with LPS or PAE. (F) CCK-8 for the detection of cell viability. (G) Cell migration evaluated with cell scratch assay. (H) Angiogenesis ability assessed by tube formation assay. Data are presented as the mean ± SD, and the experiments were repeated three times, $^{*}P < 0.05$, $^{**}P < 0.01$, $^{***}P < 0.001$.

trations of PAE (Figs. 2C, 2D, and S1A). Similarly, *LINC01133* and *SLAMF9* mRNA levels increased in LPS-treated cells but decreased with higher PAE concentrations (Fig. 2E). An optimal PAE concentration of 20 μg·mL^{-1} was selected for further experiments. Subsequently, LPS-induced macrophages were co-cultured with HUVECs and treated with PAE. In the LPS-exposed cells, HUVEC viability, migration, and angiogenesis were significantly inhibited compared to the control group. However, these effects were alleviated by PAE treatment (Figs. 2F−2H). In conclusion, PAE effectively suppresses M1 macrophage polarization and promotes HUVEC proliferation, migration, and angiogenesis.

PAE regulates macrophage polarization, HUVEC proliferation, migration, and angiogenesis by downregulating LINC01133 and SLAMF9

To elucidate the molecular mechanisms underlying PAE's effects, we examined its impact on *LINC01133* and *SLAMF9* expressions. PAE treatment resulted in decreased levels of *LINC01133* and *SLAMF9*. Conversely, transfection with Oe-*LINC01133* or Oe-*SLAMF9* upregulated these genes (Figs. 3A and 3B). In LPS-stimulated macrophages, PAE reduced the expression of CD86, IL-6, and TNF-α. However, these effects were mitigated by overexpression of *LINC01133* or *SLAMF9* (Figs. 3C, S1B and 3D). Furthermore, PAE-enhanced HUVEC viability, migration, and angiogenesis were inhibited by the overexpression of *LINC01133* or *SLAMF9* (Figs. 3E−3G). These results suggest that PAE modulates macrophage polarization and HUVEC functions by downregulating *LINC01133* and *SLAMF9*.

LINC01133 upregulates SLAMF9 expression through interaction with ELAVL1

Next, we explored whether *LINC01133* influences wound healing in infectious diabetic ulcers by regulating *SLAMF9* expression. A positive correlation between *LINC01133* and *SLAMF9* expressions was observed in wound tissues from diabetic anal fistula patients (Fig. 4A). Starbase predicted *ELAVL1* was a common RBP for both *LINC01133* and *SLAMF9*. This prediction was experimentally verified through RNA immunoprecipitation, which showed increased *LINC01133* enrichment in the anti-*ELAVL1* group compared to the IgG group (Fig. 4B). RNA pull-down assays demonstrated that *ELAVL1* was more abundantly pulled down in the Bio-*SLAMF9* group than in the Bio-NC group (Fig. 4C). Overexpression of *LINC01133* in HUVECs led to increased levels of *LINC01133*, *ELAVL1* and *SLAMF9* levels, whereas *ELAVL1* knockdown reduced *ELAVL1* and *SLAMF9* levels without affecting *LINC01133* expression (Figs. 4D and 4E). To assess the role of *LINC01133* in *SLAMF9* mRNA stability, HUVECs were treated with actinomycin D. Overexpression of *LINC01133* slowed *SLAMF9* mRNA degradation compared to the Oe-NC group, while *ELAVL1* knockdown accelerated *SLAMF9* mRNA degradation (Fig. 4F). These findings indicate that *LINC01133* interacts with *ELAVL1* to stabilize and upregulate *SLAMF9* expression.

Overexpression of SLAMF9 mitigates the effects of LINC01133 silencing on macrophage polarization, HUVEC proliferation, migration, and angiogenesis

To investigate the roles of *LINC01133* and *SLAMF9* in macrophage polarization, macrophages were transfected with sh-*LINC01133* or Oe-*SLAMF9* and subsequently treated with LPS. Silencing *LINC01133* reduced the expression levels of both *LINC01133* and *SLAMF9* in LPS-exposed macrophages, while overexpressing *SLAMF9* increased *SLAMF9* level without affecting *LINC01133* (Figs. 5A and 5B). *LINC01133* knockdown led to decreased levels of CD86, TNF-α, and IL-6, which were reversed by *SLAMF9* overexpression (Figs. 5C, S1C, and 5D). The roles of *LINC01133* and *SLAMF9* in HUVEC proliferation, migration, and angiogenesis were also examined. Macrophages transfected with sh-*LINC01133* or Oe-*SLAMF9* were co-cultured with HUVECs. Results indicated that *LINC01133* knockdown enhanced HUVEC viability, migration, and angiogenesis, whereas these enhancements were mitigated by *SLAMF9* overexpression (Figs. 5E−5G). These findings suggest that *SLAMF9* overexpression counteracts the effects of *LINC01133* knockdown on macrophage polarization, as well as HUVEC proliferation, migration, and angiogenesis.

Discussion

Diabetic ulcers represent a significant and challenging complication of diabetes mellitus, with current treatments often failing to produce satisfactory outcomes [31]. Thus, the identification of effective therapeutics to enhance diabetic wound healing is both urgent and essential [32]. This study demonstrated that PAE suppressed M1 macrophage polarization and promoted HUVEC proliferation, migration, and angiogenesis. Notably, we identified the regulation of the *LINC01133*/*ELAVL1*/*SLAMF9* axis in macrophages as a potential mechanism by which PAE facilitates wound healing in infectious diabetic ulcers.

Although previous studies have confirmed the protective effects of PAE in diabetic wound healing, the underlying molecular mechanisms remain unclear. PAE has demonstrated efficacy in ameliorating dextran sulfate sodium-induced ulcerative colitis [33] and promoting hard palate mucosal wound healing through the PI3K/AKT signaling pathway [34]. lncRNAs are known to play critical roles in key processes of diabetic wound healing, including inflammation, angiogenesis, and extracellular matrix remodeling [35, 36]. However, the involvement of lncRNAs in PAE-mediated wound healing has not been fully explored. In this study, we collected wound tissues from diabetic anal fistula patients with or without PAE treatment and performed high-throughput sequencing to identify differentially expressed lncRNAs. Our findings represent the first validation of *LINC01133* downregulation in wound tissues and PBMCs from PAE-treated diabetic anal fistula patients. Additionally, we demonstrated that PAE treatment reduced *LINC01133* expression in LPS-exposed macrophages derived from the PBMCs of these patients.

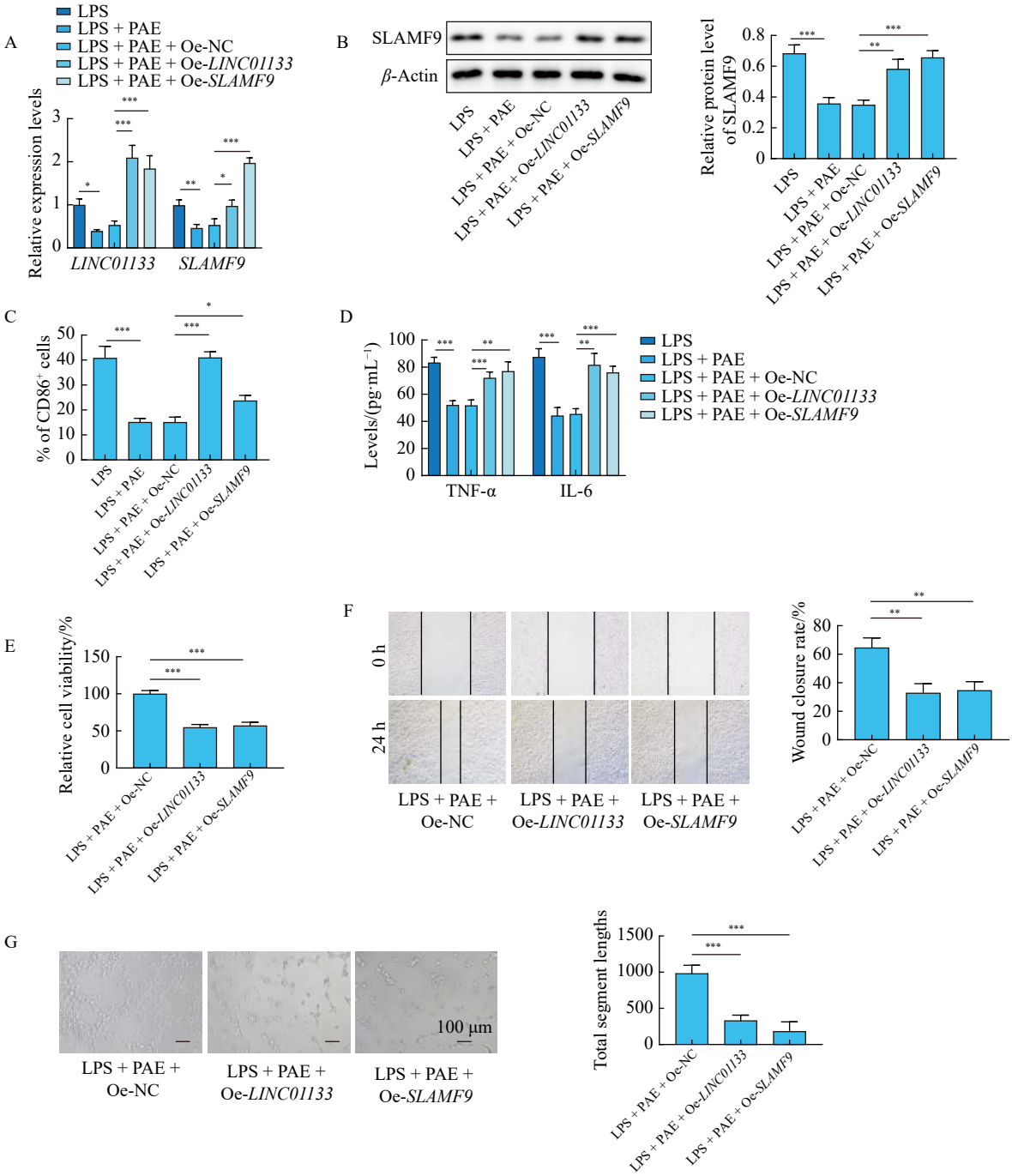

Fig. 3 PAE downregulated *LINC01133* and *SLAMF9* to inhibit M1 macrophage polarization and promote HUVEC proliferation, migration, and angiogenesis. (A−D) Macrophages were transfected with Oe-NC, Oe-*LINC01133*, or Oe-*SLAMF9*, followed by LPS or PAE treatment. *LINC01133* and *SLAMF9* mRNA were determined (A). SLAMF9 protein level was detected (B). CD86 was identified using flow cytometry (C). ELISA for detecting TNF-α and IL-6 (D). (E−G) HUVEC were co-cultured with macrophages, followed by transfected with Oe-NC or Oe-*LINC01133*. Then cells were added with LPS or PAE. (E) CCK-8 for detecting cell viability. (F) Cell migration detected by cell scratch assay. (G) The assessment of angiogenesis ability. Data are presented as the mean ± SD, and the experiments were repeated three times, $^{*}P < 0.05$, $^{**}P < 0.01$, $^{***}P < 0.001$.

LINC01133 is a well-characterized lncRNA implicated in the malignancy of various cancers, including those affecting the urinary, respiratory, and digestive systems [37]. It has been shown to facilitate the progression of cervical cancer [38] and serves as a potential biomarker for diagnosing cervical squamous carcinoma [39]. Importantly, our results indicate that overexpression of *LINC01133* diminishes the inhibitory effect of PAE on M1 macrophage polarization and the promotive effect of PAE on HUVEC proliferation, migration, and angiogenesis. These findings suggest that PAE enhances dia-

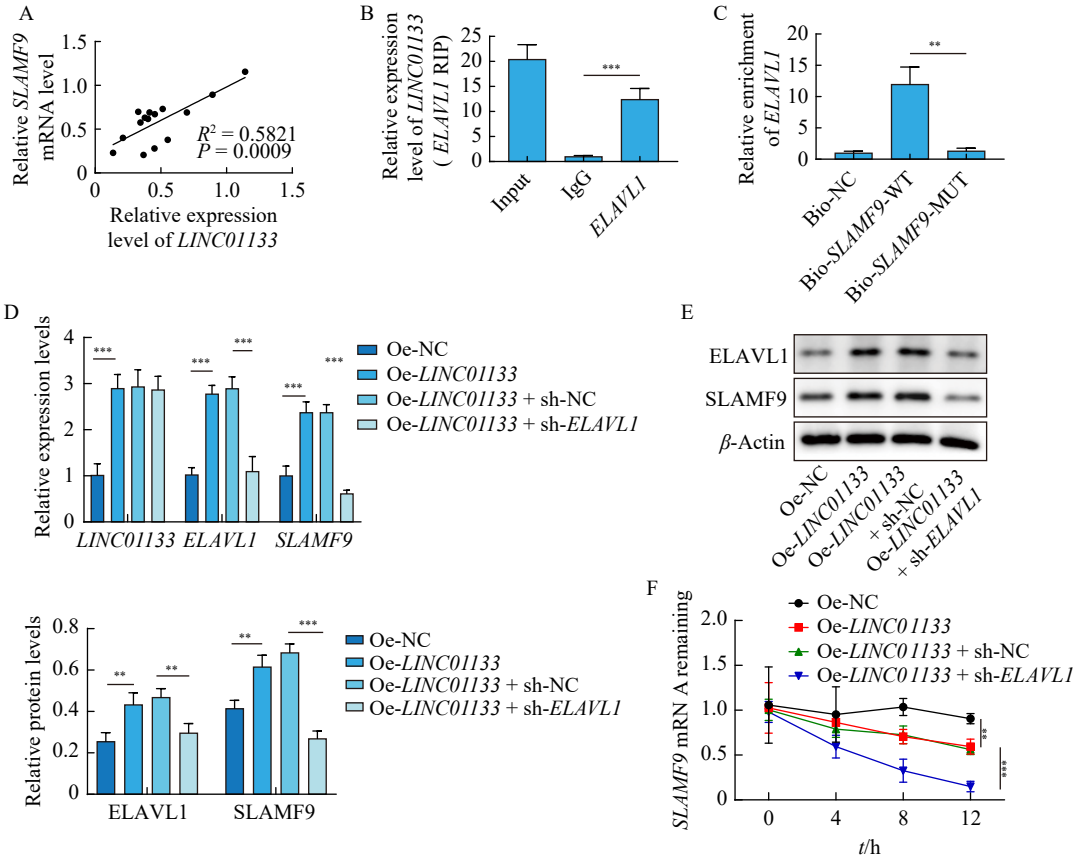

Fig. 4 *LINC01133* upregulated *SLAMF9* expression through *ELAVL1*. (A) Correlation analysis of the expressions of *LINC01133* and *SLAMF9*. (B) The regulatory relationship of *LINC01133* and *ELAVL1* was determined by RNA immunoprecipitation in HEK293 cells. (C) The interaction of *ELAVL1* and *SLAMF9* was detected by RNA pull-down in HEK293 cells. (D, E) HUVEC were transfected with Oe-NC, Oe-*LINC01133*, sh-NC or sh-*ELAVL1*. *LINC01133* and the mRNA levels of *ELAVL1* and *SLAMF9* were determined by RT-qPCR (D). ELAVL1 and SLAMF9 protein levels were measured using western blot (E). (F) HUVEC transfected with Oe-NC, Oe-*LINC01133*, sh-NC, or sh-*ELAVL1* were treated with actinomycin D (2 mg·μL^{-1}) for 0, 4, 8 and 12 h. *SLAMF9* mRNA was then determined by RT-qPCR. Data are presented as the mean ± SD and the experiments were repeated three times, $^{**}P < 0.01$, $^{***}P < 0.001$.

betic wound healing by modulating *LINC01133* expression. Moreover, our study highlights the potential role of *LINC01133* in the wound healing process of infectious diabetic ulcers. Further research is warranted to elucidate the specific mechanisms by which PAE regulates *LINC01133* expression. Macrophages play a pivotal role in wound healing and angiogenesis, with M2 macrophages exhibiting anti-inflammatory and pro-angiogenic properties, while M1 macrophages are pro-inflammatory [40]. Diabetic wounds are characterized by persistent and dysregulated M1 macrophage polarization [41]. Our study demonstrated that PAE treatment reduces M1 macrophage levels in PBMCs from diabetic anal fistula patients. Furthermore, PAE suppressed M1 macrophage polarization and inflammatory cytokine release, and it enhanced HUVEC proliferation, migration, and angiogenesis in co-cultures with LPS-induced macrophages. Furthermore, PAE suppressed M1 macrophage polarization and inflammatory cytokine release, and it enhanced HUVEC proliferation, migration, and angiogenesis in co-cultures with LPS-induced macrophages. Finally, we investigated the downstream regulatory mechanisms of *LINC01133* in macrophages.

SLAMF9 has been shown to delay wound closure in macrophage-like cells and enhance the secretion of TNF-α following LPS stimulation [23]. It plays a crucial role in the production of pro-inflammatory cytokines in monocyte cell lines, such as THP-1 cells [21]. Additionally, *SLAMF9* is upregulated in macrophages and regulatory macrophages (R-Mϕs) in diffuse cutaneous leishmaniasis [42]. In this study, we found that *SLAMF*9 was downregulated in wound tissues and PBMCs from PAE-treated diabetic anal fistula patients. Moreover, PAE decreased *SLAMF9* levels in LPS-exposed macrophages derived from these PBMCs. To our knowledge, this is the first report demonstrating that PAE downregulates *SLAMF9* expression both in clinical samples and *in vitro*. Importantly, we validated that PAE exerted regulatory effects on macrophages and HUVEC by downregulating *LINC01133* and *SLAMF9*.

ELAVL1 is a widely expressed RBP that modulates RNA stability and protein expression [43]. For example, lncRNA *HOXB-AS1* recruits *ELAVL1* to enhance the mRNA stability

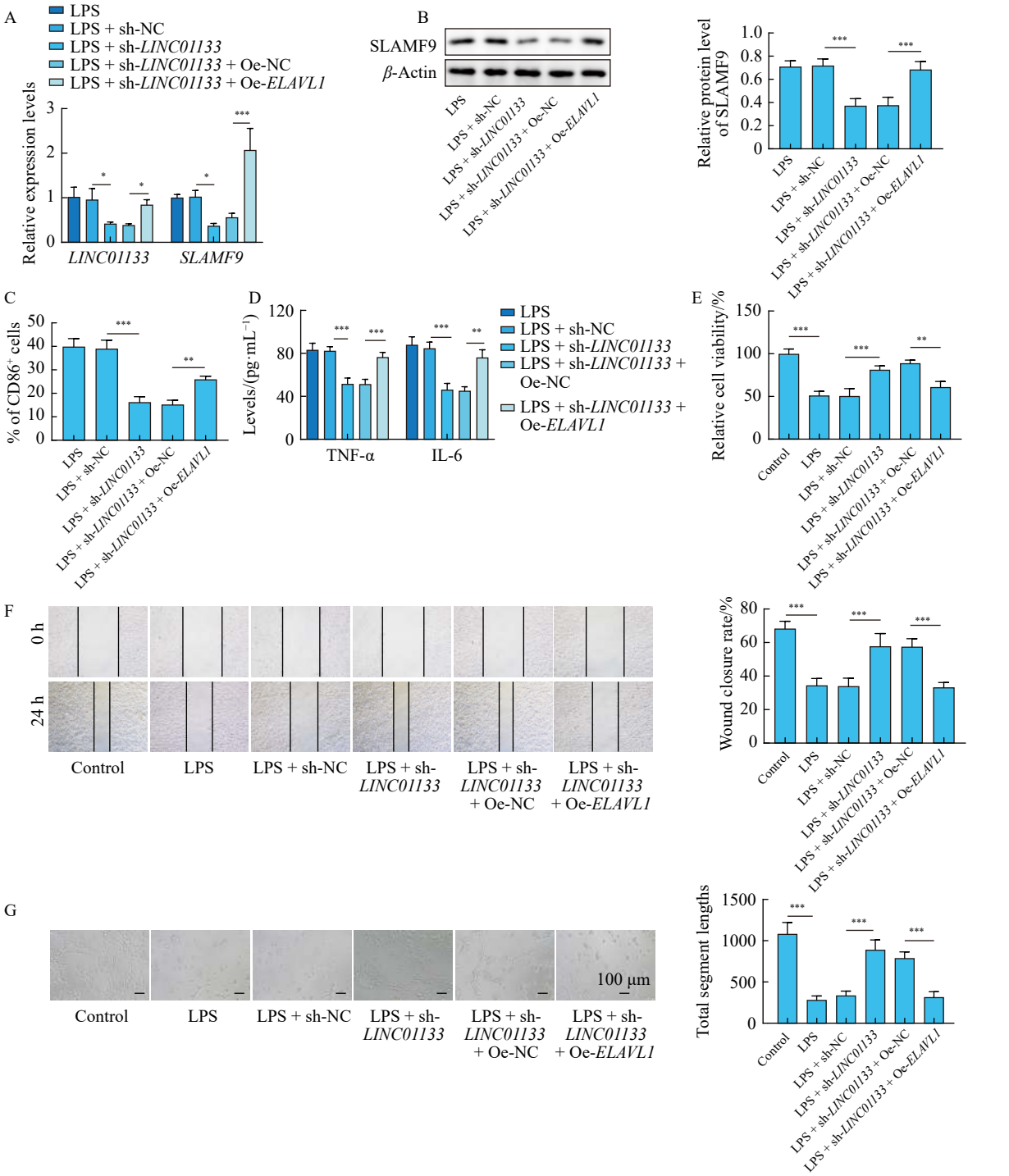

Fig. 5 Overexpression of *SLAMF9* overturned the effect of *LINC01133* knockdown on macrophage polarization, HUVEC proliferation, migration, and angiogenesis. (A−D) Macrophages transfected with sh-NC, sh-*LINC01133*, Oe-NC, or Oe-*SLAMF9* were added with LPS. *LINC01133* and *SLAMF9* mRNA were detected (A). SLAMF9 protein expression was detected (B). CD86 was identified by flow cytometry (C). ELISA for measuring TNF-α and IL-6 (D). (E−G) HUVEC were co-cultured with macrophages, followed by transfected with sh-NC, sh-*LINC01133*, Oe-NC, or Oe-*SLAMF9*. Then cells were added with LPS. CCK-8 for detecting cell viability (E). Cell scratch assay for cell migration (F). The assessment of angiogenesis ability (G). Data are presented as the mean ± SD, and the experiments were repeated three times, $^{*}P < 0.05$, $^{**}P < 0.01$, $^{***}P < 0.001$.

of fucosyltransferase 4 (*FUT4*) in multiple myeloma [44], and lncRNA *B4GALT1-AS1* binds to *ELAVL1* to stabilize the mRNA of yes-associated protein (*YAP*) and enhance its transcriptional activity in osteosarcoma [45]. Starbase predictions suggest that *ELAVL1* is a common RBP for both *LINC01133* and *SLAMF9*. *ELAVL1* is implicated in various diabetes-re-

lated diseases, including diabetic cardiomyopathy and diabetic nephropathy [25, 26]. Knockdown of *ELAVL1* mimics anti-inflammatory effects and attenuates inflammatory response post-myocardial infarction [46], making *ELAVL1* a potential therapeutic target for macrophage-related pathologies [47]. Our study confirmed the direct interactions between *ELAVL1* and both *LINC01133* and *SLAMF9* through RNA immunoprecipitation and RNA pull-down assays. Importantly, this is the first research to validate that *LINC01133* interacts with *ELAVL1* to upregulate *SLAMF9*. We also found that the knockdown of *LINC01133* inhibited M1 macrophage polarization and improved HUVEC proliferation, migration, and angiogenesis through the downregulation of *SLAMF9*. This finding suggests that the regulation of the *LINC01133*/*SLAMF9* axis in macrophages is a critical mechanism mediating the effects of PAE.

Our results demonstrated that *LINC01133* and *SLAMF9* expressions decreased in diabetic anal fistula patients treated with PAE. PAE suppressed M1 macrophage polarization and promoted HUVEC proliferation, migration, and angiogenesis by downregulating *LINC01133*/*SLAMF9*. Additionally, *LINC01133* upregulated *SLAMF9* through interaction with *ELAVL1* in macrophages. These findings provide a novel perspective on the molecular mechanisms underlying the efficacy of PAE in promoting wound healing in infectious diabetic ulcers.

References

[1] Golledge J, Thanigaimani S. Novel therapeutic targets for diabetes-related wounds or ulcers: an update on preclinical and clinical research [J]. *Expert Opin Ther Targets*, 2021, **25**(12): 1061-1075.

[2] Everett E, Mathioudakis N. Update on management of diabetic foot ulcers [J]. *Ann N Y Acad Sci*, 2018, **1411**(1): 153-165.

[3] El-Ashram S, El-Samad LM, Basha AA, *et al*. Naturally-derived targeted therapy for wound healing: beyond classical strategies [J]. *Pharmacol Res*, 2021, **170**: 105749.

[4] Aitcheson SM, Frentiu FD, Hurn SE, *et al*. Normal macrophage function and macrophage dysfunction in diabetic wounds [J]. *Molecules*, 2021, **26**(16): 4917.

[5] Chang M, Nguyen TT. Strategy for treatment of infected diabetic foot ulcers [J]. *Acc Chem Res*, 2021, **54**(5): 1080-1093.

[6] Louiselle AE, Niemiec SM, Zgheib C, *et al*. Macrophage polarization and diabetic wound healing [J]. *Transl Res*, 2021, **236**: 109-116.

[7] Pang L, Liao Q, Zou L, *et al*. Two glycoproteins from medicinal insect *Periplaneta americana* (L.) promote diabetic wound healing *via* macrophage polarization modulation [J]. *Int J Biol Macromol*, 2022, **209**: 2130-2141.

[8] Liao Q, Pang L, Li JJ, *et al*. Characterization and diabetic wound healing benefits of protein-polysaccharide complexes isolated from an animal ethno-medicine *Periplaneta americana* L. [J]. *Int J Biol Macromol*, 2022, **195**: 466-474.

[9] Yuan H, Su J, Tan J, *et al*. Efficacy of Kangfuxin Liquid on radiotherapy-induced oral mucositis for patients with head and neck squamous cell carcinoma and its effect on salivary glands and immune function [J]. *Am J Transl Res*, 2022, **14**(9): 6792-6804.

[10] Wan X, Gen F, Sheng Y, *et al*. Meta-analysis of the effect of Kangfuxin Liquid on diabetic patients with skin ulcers [J]. *Evid Based Complement Alternat Med*, 2021, **2021**: 1334255.

[11] Lu S, Wu D, Sun G, *et al*. Gastroprotective effects of Kangfuxin against water-immersion and restraint stress-induced gastric ulcer in rats: roles of antioxidation, anti-inflammation, and pro-survival [J]. *Pharm Biol*, 2019, **57**(1): 770-777.

[12] Chen P, Shen Y, Shi H, *et al*. Gastroprotective effects of Kangfuxin-against ethanol-induced gastric ulcer *via* attenuating oxidative stress and ER stress in mice [J]. *Chem Biol Interact*, 2016, **28**: S0009-2797(16)30509-9.

[13] Kuai L, Jiang JS, Li W, *et al*. Long non-coding RNAs in diabetic wound healing: current research and clinical relevance [J]. *Int Wound J*, 2022, **19**(3): 583-600.

[14] Hu J, Zhang L, Liechty C, *et al*. Long non-coding RNA *GAS5* regulates macrophage polarization and diabetic wound healing [J]. *J Invest Dermatol*, 2020, **140**(8): 1629-1638.

[15] Li B, Zhou Y, Chen J, *et al*. Long non-coding RNA *H19* contributes to wound healing of diabetic foot ulcer [J]. *J Mol Endocrinol*, 2020, **1**: JME-19-0242.R1.

[16] Li Z, Xu D, Chen X, *et al*. *LINC01133*: an emerging tumor-associated long non-coding RNA in tumor and osteosarcoma [J]. *Environ Sci Pollut Res Int*, 2020, **27**(26): 32467-32473.

[17] Yang XZ, Cheng TT, He QJ, *et al*. *LINC01133* as ceRNA inhibits gastric cancer progression by sponging miR-106a-3p to regulate APC expression and the Wnt/beta-catenin pathway [J]. *Mol Cancer*, 2018, **17**(1): 126.

[18] Zhang W, Du M, Wang T, *et al*. Long non-coding RNA *LINC01133* mediates nasopharyngeal carcinoma tumorigenesis by binding to *YBX1* [J]. *Am J Cancer Res*, 2019, **9**(4): 779-790.

[19] Cannons JL, Tangye SG, Schwartzberg PL. SLAM family receptors and SAP adaptors in immunity [J]. *Annu Rev Immunol*, 2011, **29**: 665-705.

[20] Dragovich MA, Mor A. The SLAM family receptors: potential therapeutic targets for inflammatory and autoimmune diseases [J]. *Autoimmun Rev*, 2018, **17**(7): 674-682.

[21] Wilson TJ, Clare S, Mikulin J, *et al*. Signalling lymphocyte activation molecule family member 9 is found on select subsets of antigen-presenting cells and promotes resistance to Salmonella infection [J]. *Immunology*, 2020, **159**(4): 393-403.

[22] Zeng X, Liu G, Peng W, *et al*. Combined deficiency of *SLAMF8* and *SLAMF9* prevents endotoxin-induced liver inflammation by downregulating *TLR4* expression on macrophages [J]. *Cell Mol Immunol*, 2020, **17**(2): 153-162.

[23] Dollt C, Michel J, Kloss L, *et al*. The novel immunoglobulin super family receptor *SLAMF9* identified in TAM of murine and human melanoma influences pro-inflammatory cytokine secretion and migration [J]. *Cell Death Dis*, 2018, **9**(10): 939.

[24] Ren Y, Yang M, Wang X, *et al*. ELAV-like RNA binding protein 1 regulates osteogenesis in diabetic osteoporosis: involvement of divalent metal transporter 1 [J]. *Mol Cell Endocrinol*, 2022, **546**: 111559.

[25] Jeyabal P, Thandavarayan RA, Joladarashi D, *et al*. MicroRNA-9 inhibits hyperglycemia-induced pyroptosis in human ventricular cardiomyocytes by targeting ELAVL1 [J]. *Biochem Biophys Res Commun*, 2016, **471**(4): 423-429.

[26] Li X, Zeng L, Cao C, *et al*. Long noncoding RNA *MALAT1* regulates renal tubular epithelial pyroptosis by modulated miR-23c targeting of *ELAVL1* in diabetic nephropathy [J]. *Exp Cell Res*, 2017, **350**(2): 327-335.

[27] Zhang L, Feng H, Jin Y, *et al*. Long non-coding RNA *LINC01119* promotes neuropathic pain by stabilizing *BDNF* transcript [J]. *Front Mol Neurosci*, 2021, **14**: 673669.

[28] Wang Z, Wang X, Zhang T, *et al*. LncRNA *MALAT1* promotes gastric cancer progression *via* inhibiting autophagic flux and inducing fibroblast activation [J]. *Cell Death Dis*, 2021, **12**(4): 368.

[29] Kang J, Liu Y, Peng S, *et al*. Efficacy and safety of traditional Chinese medicine external washing in the treatment of post-operative wound of diabetes complicated with anal fistula: study protocol of a randomized, double-blind, placebo-controlled, multi-center clinical trial [J]. *Front Pharmacol*, 2022, **13**: 938270.
[30] Lotfollahi Z, Dawson J, Fitridge R, *et al*. The anti-inflammatory and proangiogenic properties of high-density lipoproteins: an emerging role in diabetic wound healing [J]. *Adv Wound Care (New Rochelle)*, 2021, **10**(7): 370-380.
[31] Zhang JJ, Zhou R, Deng LJ, *et al*. Huangbai liniment and berberine promoted wound healing in high-fat diet/streptozotocin-induced diabetic rats [J]. *Biomed Pharmacother*, 2022, **150**: 112948.
[32] Patel S, Srivastava S, Singh MR, *et al*. Mechanistic insight into diabetic wounds: pathogenesis, molecular targets and treatment strategies to pace wound healing [J]. *Biomed Pharmacother*, 2019, **112**: 108615.
[33] Ni L, Lu Q, Tang M, *et al*. *Periplaneta americana* extract ameliorates dextran sulfate sodium-induced ulcerative colitis *via* immunoregulatory and PI3K/AKT/NF-kappaB signaling pathways [J]. *Inflammopharmacology*, 2022, **30**(3): 907-918.
[34] Zhao B, Xu J, Wang Y, *et al*. *Periplaneta americana* extract promotes hard palate mucosal wound healing *via* the PI3K/AKT signaling pathway in male mice [J]. *Arch Oral Biol*, 2024, **158**: 105856.
[35] Li J, Wei M, Liu X, *et al*. The progress, prospects, and challenges of the use of non-coding RNA for diabetic wounds [J]. *Mol Ther Nucleic Acids*, 2021, **24**: 554-578.
[36] Li X, Li N, Li B, *et al*. Noncoding RNAs and RNA-binding proteins in diabetic wound healing [J]. *Bioorg Med Chem Lett*, 2021, **50**: 128311.
[37] Jiang S, Zhang Q, Li J, *et al*. New sights into long non-coding RNA *LINC01133* in cancer [J]. *Front Oncol*, 2022, **12**: 908162.
[38] Feng Y, Qu L, Wang X, *et al*. *LINC01133* promotes the progression of cervical cancer by sponging miR-4784 to up-regulate *AHDC1* [J]. *Cancer Biol Ther*, 2019, **20**(12): 1453-1461.
[39] Wang WJ, Wang D, Zhao M, *et al*. Serum lncRNAs (*CCAT2*, *LINC01133*, *LINC00511*) with squamous cell carcinoma antigen panel as novel non-invasive biomarkers for detection of cervical squamous carcinoma [J]. *Cancer Manag Res*, 2020, **12**: 9495-9502.
[40] Chambers SE, O'Neill CL, O'Doherty TM, *et al*. The role of immune-related myeloid cells in angiogenesis [J]. *Immunobiology*, 2013, **218**(11): 1370-1375.
[41] Wolf SJ, Melvin WJ, Gallagher K. Macrophage-mediated inflammation in diabetic wound repair [J]. *Semin Cell Dev Biol*, 2021, **119**: 111-118.
[42] Christensen SM, Belew AT, El-Sayed NM, *et al*. Host and parasite responses in human diffuse cutaneous leishmaniasis caused by *L. amazonensis* [J]. *PLoS Negl Trop Dis*, 2019, **13**(3): e0007152.
[43] Liu R, Wu K, Li Y, *et al*. Human antigen R: a potential therapeutic target for liver diseases [J]. *Pharmacol Res*, 2020, **155**: 104684.
[44] Chen R, Zhang X, Wang C. LncRNA *HOXB-AS1* promotes cell growth in multiple myeloma *via* FUT4 mRNA stability by ELAVL1 [J]. *J Cell Biochem*, 2020, **121**(10): 4043-4051.
[45] Li Z, Wang Y, Hu R, *et al*. LncRNA *B4GALT1-AS1* recruits HuR to promote osteosarcoma cells stemness and migration *via* enhancing YAP transcriptional activity [J]. *Cell Prolif*, 2018, **51**(6): e12504.
[46] Krishnamurthy P, Lambers E, Verma S, *et al*. Myocardial knockdown of mRNA-stabilizing protein *HuR* attenuates post-MI inflammatory response and left ventricular dysfunction in IL-10-null mice [J]. *FASEB J*, 2010, **24**(7): 2484-2494.
[47] Nagai N, Kawashima H, Toda E, *et al*. Renin-angiotensin system impairs macrophage lipid metabolism to promote age-related macular degeneration in mouse models [J]. *Commun Biol*, 2020, **3**(1): 767.

Cite this article as: YANG Yuhang, HUANG Jun, LI Xintian, *et al*. *Periplaneta americana* extract promotes infectious diabetic ulcers wound healing by downregulation of *LINC01133*/*SLAMF9* [J]. *Chin J Nat Med*, 2024, **22**(7): 608-618.